

Chapter

4. Structural Features

4.1 Introduction

Studies of changes in the structural features of polymers, such as chemical composition, morphology, and molecular weight distribution induced by environmental exposure are numerous. However, in the case of polycarbonate, there is a distinct lack of agreement concerning the area of the chemical mechanisms governing the degradation. While the specifics of the chemistry is tangential to the main thrust of this work, some evidence will be presented to bolster one or the other of the two common theories relevant to PC degradation which are put forth in the literature today. The primary goal in this present study is to relate thermally induced degradation to primary parameters, such as molecular weight distribution.

Through an examination of the thermally induced changes in polypropylene, Chan and Balke^{1,2,3} showed the novel possibilities of MWD/degradation superposition. This was demonstrated by showing that MWDs for two samples with the same degree of degradation, but different thermal histories, were identical. Modeling of this phenomenon is predicated upon application of a quantity τ , the degree of degradation which is defined as the product of the kinetic rate constant, k and the time of degradation, t . These researchers used gel permeation chromatography results to calculate τ based on the fact that the reactions occurring in polypropylene are well-known and can be described in terms of chain length changes (see Chapter 1). However, for a complex heteroatom polymer such as polycarbonate, where the degradation reaction mechanisms are not known with any certainty, TGA provides perhaps the only way to measure a value for k , albeit in an indirect manner. Clearly, GPC results are more directly related to

¹ Chan, J. H. and S. T. Balke, *Polym. Degrad. Stab.*, **57**, 113, 1997.

² Chan, J. H. and S. T. Balke, *Polym. Degrad. Stab.*, **57**, 127, 1997.

³ Chan, J. H. and S. T. Balke, *Polym. Degrad. Stab.*, **57**, 135, 1997.

changes in chain length than are data from isothermal TGA measurements, which will be utilized in the present study. Until such time as the degradation mechanisms are more fully known, these MWD measurements are the best descriptors of molecular level processes in PC degradation.

Since this methodology of MWD superposition has not been reported elsewhere, verification of these results for other polymers was the next logical step. The current study applies this technique to a commercial bisphenol A polycarbonate, PC(Lex) (Lexan®, General Electric), as well as to a similar material which is a laboratory grade with no stabilizer chemicals added, PC(Lab). These materials have been previously studied to ascertain their kinetic behavior (see Chapter 3), so values for the degradation rate constant, k , are readily known. It remained, then, to thermally degrade the materials for specified times to achieve particular levels of modification. Then the resulting samples were analyzed for molecular weight distribution as described above. While recognizing the power of the methodology, Chan and Balke stopped short of developing a master curve for these molecular weight distributions. This study extends their work.

4.2 Degradation Conditions

Much of the present research has focused on the laboratory grade polymer, with a limited analysis of the commercial material to strengthen the conclusions. In both cases, polymer pellets were first dried in a vacuum oven overnight at a temperature of approximately 120°C, as recommended by General Electric. If the material was not immediately used, it was stored in a dessicator to minimize moisture absorption, which can affect the mechanism of the degradation. The degradations were carried out in a specially designed chamber consisting of a 4" threaded pipe nipple with two endcaps. The upper cap was drilled with holes so that a gas purge line could be introduced, thereby controlling the atmosphere of the chamber. The entire assembly, shown schematically in Figure 4.3.1-1, contained an aluminum pan holding the dried pellets, and was placed in an oven and purged for about 30 minutes with nitrogen at a flow rate of 18 mL/min prior to heating. This operation displaced much of the air in the cell to ensure a primarily nitrogen atmosphere for the degradation. Next, the oven was ramped at the fastest rate possible (approximately 15°C/min) to the desired temperature (325, 350, 375, or 400°C)

and held for a specified time. This timing was started when the oven indicated 300°C since it is reported that no appreciable degradation occurs below this temperature. When the time had elapsed, the oven temperature was lowered as quickly as possible and the sample removed. The aluminum pan was then simply peeled off, leaving solid polymer resembling a hockey puck, which could then be compression molded for further testing.

For this study the initial sample geometry was pellets. However, the degradation temperatures are high enough that the sample is no longer solid and can thus flow and consolidate into a single piece. This renders the initial geometry irrelevant. The only geometric factors of concern would be transfer of any volatile products out of the center of the sample, which would clearly be a faster process for a thinner piece of material. However, in this study, all samples were approximately the same mass, which should then normalize this process across all samples. Additionally, once the consolidated polymer was pressed into films, there was no evidence, except for the expected edge effects where the material contacted the aluminum dish, that any inhomogeneity existed within the sample.

In compression molding, the solid polymer was placed between two sheets of teflon and pressed at 260°C to flatten it. It was then pressed again at 260°C using a picture frame mold with a thickness of 0.2 mm and at a maximum pressure of 4000 pounds. The sample experienced a total time of approximately 22 minutes within the press. However, since 260°C is lower than the minimum temperature for any readily observable degradation, this should not increase the level of degradation of the samples. If slight changes did occur they should be constant from sample to sample.

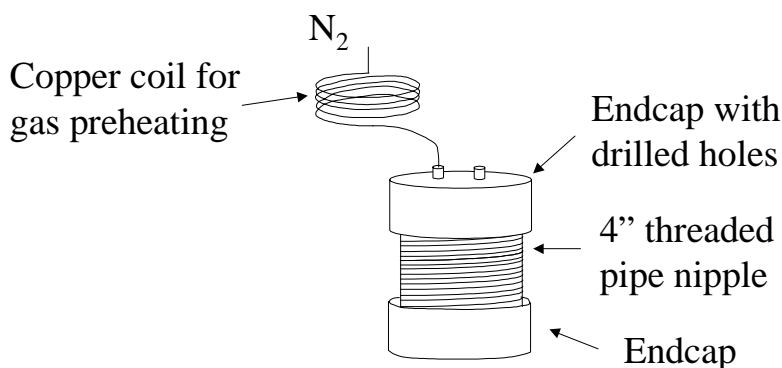


Figure 4.3.1-1 Schematic representation of the degradation chamber utilized in this study.

During the degradation step, the oven temperature is certainly not that of the sample due to thermal lag effects, so a test was devised whereby this difference could be accounted for and corrections made. A thermocouple was placed through the third hole in the upper endcap and into the sample pan. Then the temperature of both the thermocouple and the oven were monitored as functions of time for each of the isotherms of interest. Not only does the sample heat at a slower rate than the oven, but it cools more slowly as well. Thus, a net thermal lag can be calculated and simply subtracted from the degradation time. A graph of this lag experiment is illustrated in Figure 4.3.1-2.

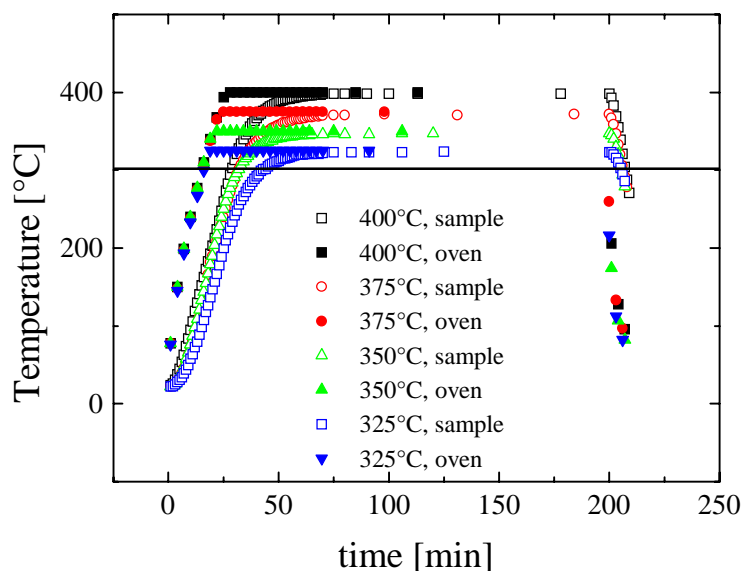


Figure 4.3.1-2 Thermal lag for isotherms during degradation in oven. Solid line represents 300°C, the temperature below which no degradation occurs. Solid symbols indicate to the oven temperature, open symbols to the sample.

This thermal lag correction to the time, t , can be combined with the reaction rate constants, k , calculated in Chapter 3 to yield values for τ . Clearly, though, it is necessary to ascertain the error in the calculation of τ . Because it is quite difficult to find an error associated with measurement of the time, and since such an error would likely be small, it was necessary to utilize the error associated with the measurement of k . In Chapter 3, it was noted that, for the highest isothermal temperature, four different samples of each

material were tested to provide an indication of the inherent uncertainty in the measurement. The standard deviation for the laboratory grade material was found to be approximately one part in eight in relation to the corresponding value of k , while that for the commercial material was about one in fifteen. A conservative estimate, then, of one eighth of the value of k was taken to be the standard deviation for that particular datum. The values of $\tau = kt$ for each of the prepared samples, as well as the associated error, are shown in Table 4.2-1.

Table 4.2-1 Summary of τ Values

Degradation Conditions	τ
PC(Lab)-325°C, 30 min	3.37e-4 (4.2e-5)
325°C, 60 min	1.46e-3 (1.8e-4)
325°C, 180 min	5.95e-3 (7.4e-4)
325°C, 360 min	1.27e-2 (1.6e-3)
325°C, 720 min	2.61e-2 (3.3e-3)
325°C, 1440 min	5.31e-2 (6.6e-3)
350°C, 30 min	3.50e-3 (4.4e-4)
350°C, 60 min	8.75e-3 (1.1e-3)
350°C, 180 min	2.98e-2 (3.7e-3)
350°C, 360 min	6.13e-2 (7.7e-3)
350°C, 720 min	1.24e-1 (1.6e-2)
350°C, 1440 min	2.50e-1 (3.1e-2)
375°C, 30 min	1.58e-2 (2.0e-3)
375°C, 60 min	3.95e-2 (4.9e-3)
375°C, 180 min	1.34e-1 (1.7e-2)
375°C, 360 min	2.76e-1 (3.5e-2)
375°C, 720 min	5.6e-1 (7.0e-2)
375°C, 1440 min	1.13 (1.4e-1)
400°C, 30 min	6.98e-2 (8.7e-3)
400°C, 60 min	1.53e-1 (1.9e-2)
400°C, 180 min	4.88e-1 (6.1e-2)
400°C, 300 min	8.23e-1 (1.0e-1)
400°C, 315 min	8.60e-1 (1.1e-1)
400°C, 330 min	9.07e-1 (1.1e-1)
400°C, 360 min	9.9e-1 (1.2e-1)
400°C, 538 min	1.49 (1.9e-1)
400°C, 720 min	1.99 (2.5e-1)
400°C, 1440 min	4.00 (0.5)
PC(Lex)- 400°C, 322	0.5 (6.3e-2)
400°C, 622 min	0.98 (0.12)
400°C, 954 min	1.5 (1.9e-1)
400°C, 1276 min	2.01 (2.5e-1)

4.3 Chemistry

As discussed in Chapter 1, two points of view exist regarding the chemistry of the degradation. Montaudo and Puglisi^{4,5,6,7} espouse an ionic viewpoint whereby PC undergoes intramolecular exchange and hydrolytic cleavage of the carbonate group. Conversely, McNeill and Rincon^{8,9} support a radical mechanism involving scission at the isopropylidene unit as well as homolytic scission at the carbonate group. While the aim of this study is not to unequivocally identify the chemical reactions, it should be a relatively simple task to provide support for one or the other. Accordingly, a few techniques for such an exercise were identified and executed.

As per the study of Montaudo et al.⁷, matrix-assisted laser desorption ionization time-of-flight spectroscopy (MALDI-TOF) was attempted with these materials using a Kratos Kompact Discovery instrument from Kratos Analytical. Samples were dissolved in tetrahydrofuran at a concentration of 10 mg/mL, and the matrix used was hydroxyphenylazobenzoic acid, 10 mg/mL in THF. The analysis performed was positive ion mode laser desorption, but, unfortunately, no satisfactory results were obtained in spite of extensive efforts. This is thought to be due to an incompatibility between the solvent and the target matrix. When the solution was applied to the matrix, it spread out such that the resulting sample was very thin and thus could not produce an adequate signal. Future work recommended in this area will address the use of alternative solvents

4.3.1 TGA-MS

Another common approach for examining chemical mechanisms is thermogravimetric analysis-mass spectroscopy (TGA-MS). A TA Instruments Hi-Res TGA 2950 and a Pfeiffer Vacuum Thermostar mass spectrometer were used for this study. In this technique, dried samples of each of the polycarbonate materials were

⁴ Montaudo, G. and C. Puglisi, in *Developments in Polymer Degradation*, N. Grassie, ED., Elsevier, London, p. 35, 1987.

⁵ Montaudo, G. and C. Puglisi, *Poly. Degrad. and Stab.*, **37**, 91, 1992.

⁶ Puglisi, C., L. Sturiale, and G. Montaudo, *Macro.*, **32**, 2194, 1999.

⁷ Puglisi, C., F. Samperi, S. Carroccio, and G. Montaudo, *Macro.*, **32**, 8821, 1999.

⁸ McNeill, I. C., and A. Rincon, *Polym. Degrad. and Stab.*, **31**, 163, 1991.

⁹ McNeill, I. C., and A. Rincon, *Polym. Degrad. and Stab.*, **39**, 13, 1993.

heated in the TGA from room temperature to 900°C in a nitrogen environment at a rate of 5°C/min. The resulting products were then analyzed via the online mass spectrometer.

The two differing reaction schemes of Montaudo and McNeill each include unique products. As seen in Chapter 1, Figures 1.3-5-8, McNeill's proposed mechanism includes the production of phenol, p-cresol, p-isopropyl phenol, p-ethyl phenol, bisphenol A, and p-vinyl phenol. From Chapter 1, Figures 1.3-9 and 1.3-10, one can see that Montaudo's mechanism leads to the production of methylphenol, isopropylidene phenol, bisphenol A, and cyclic dimer and trimer. Unfortunately, however, these molecules are too large to be detected by the TGA-MS, but another product, phenol, is detectable. The resulting mass spectra for both PC(Lab) and PC(Lex), shown in Figure 4.3.1-1 and Figure 4.3.1-2, indicate the presence of p-cresol (peak at 107 amu), p-isopropyl phenol (121, 136 amu), p-ethyl phenol (107, 122 amu), and p-vinyl phenol (91, 120 amu), all of which follow from McNeill's proposed pathway. However, phenol, a product of both mechanisms, is also present with fragments at 39, 66, and 94 amu. From these data, then, it is not possible to support either mechanism. The results are consistent with McNeill's mechanism, but Montaudo's mechanism cannot be excluded. One point to note here, is that, for PC(Lab), it seems that the phenol fragments appear at a slightly earlier time than the other molecules present, which may indicate that two mechanisms are indeed at work. However, lower molecular weight products might be expected to appear earlier due to the decreasing volatility with increasing molecular weight. For PC(Lex), though, all the molecules seem to fragment at about the same time which is most likely due to the presence of stabilizers.

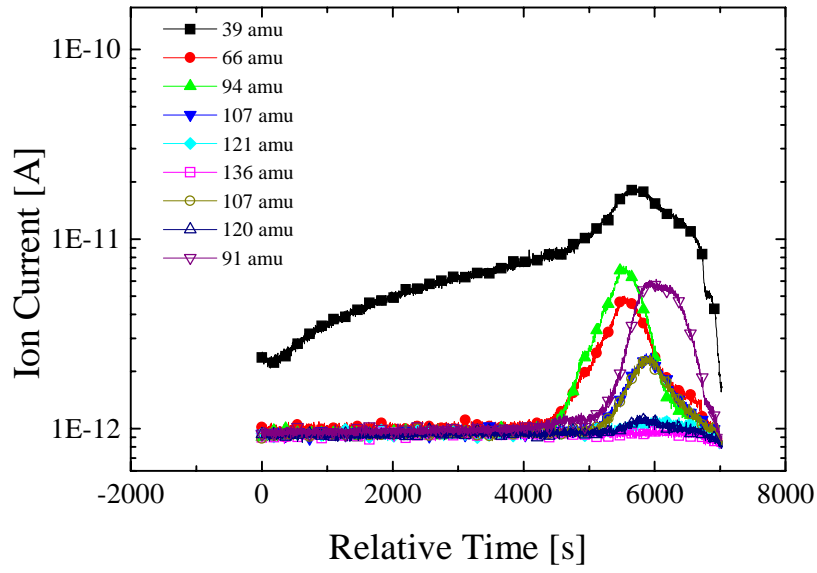


Figure 4.3.1-1 Mass spectrum for PC(Lab).

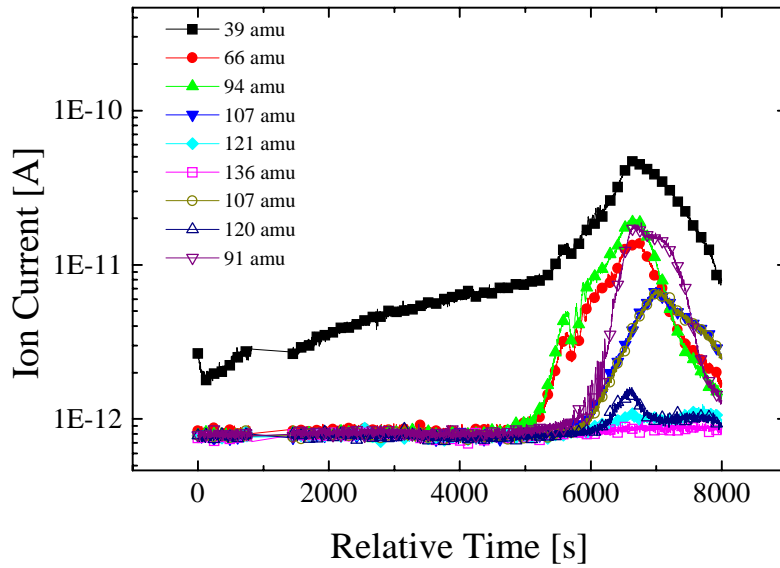


Figure 4.3.1-2 Mass spectra for PC(Lex).

4.3.2 FTIR

One additional analytical method was applied to this system, that of Fourier transform infrared spectroscopy (FTIR). The original experimental plan called for dissolution of a polymer sample in a solvent followed by attenuated total reflectance (ATR) of the solution in a trough attachment. Such a technique alleviates the necessity of identifying a reference peak (one not changing in intensity or position) by which to scale the spectra and eliminate thickness effects. It was found that this method was not viable due to the fact that the solvent signal overwhelmed that of the polymer, yielding no useful results. As an alternative, it was decided to test the polymer in solid form in an absorbance mode, which does require identification of a reference peak. For this purpose, a peak which does not undergo any changes with degradation was needed. The peak selected was that at approximately 1508 cm^{-1} , corresponding to a “semicircle” ring stretch¹⁰. Other workers¹⁰ did not see any significant changes here, particularly at the lowest degradation temperatures, and it is expected that the rings would not be directly involved in the chemical changes occurring with degradation.

In order to carry out these experiments, pieces of the thin films of both PC(Lab) and PC(Lex) were dissolved overnight in methylene chloride at a concentration of 0.025 g/mL. These solutions were then cast on KBr discs and dried under vacuum at approximately 120°C to eliminate solvent. Samples were then scanned 32 times at a resolution of 4 cm^{-1} . For PC(Lab), the neat material was scanned, as were samples degraded at: 375°C , 1 hour ($\tau = 3.95\text{e-}2$); 375°C , 6 hr ($\tau = 2.76\text{e-}1$); 400°C , 3 hr ($\tau = 4.88\text{e-}1$); and 400°C , 6 hr ($\tau = 9.9\text{e-}1$). For PC(Lex), solutions of all five samples were attempted, but only those for the neat material, for the samples degraded at 400°C , 322 min ($\tau = 0.5$) and at 400° , 622 min ($\tau = 0.98$) fully dissolved. For the two samples of higher degree of degradation (400°C , 954 min- $\tau = 1.5$ and 400°C , 1276 min, $\tau = 2.01$), the polymer would not completely dissolve in the solvent. At these extreme conditions, this could be due to either char formation or to possible crosslinking of the material. Complete spectra for both grades of polycarbonate are shown in Figure 4.3.2-1 and Figure 4.3.2-2.

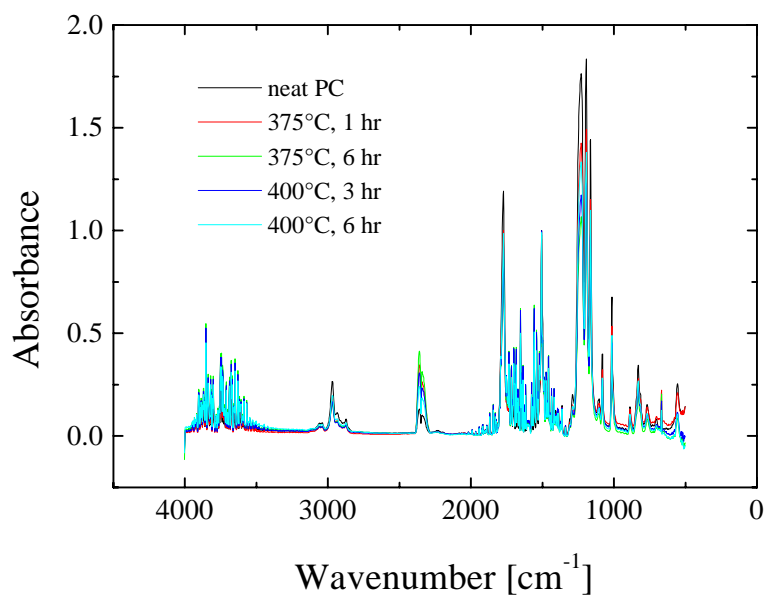


Figure 4.3.2-1 Infrared spectra for PC(Lab).

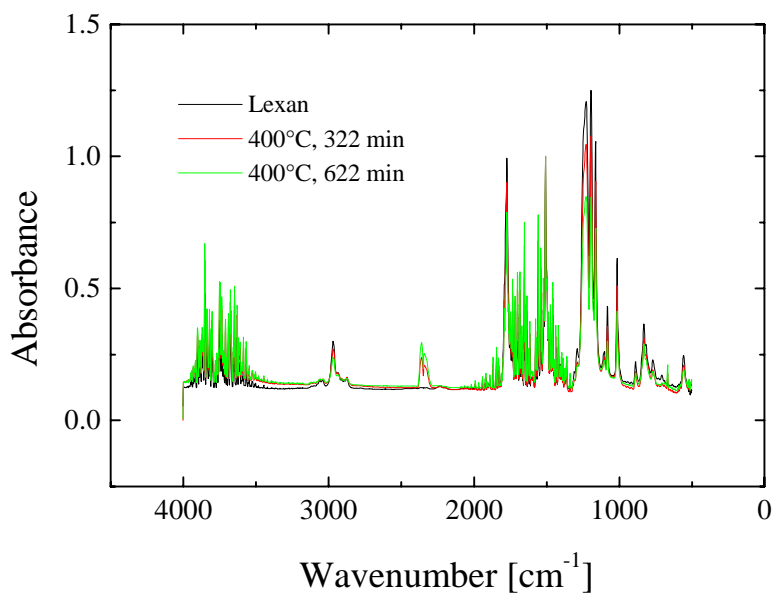


Figure 4.3.2-2 Infrared spectra for PC(Lex).

Politou and coworkers¹⁰ utilized a similar technique, photothermal beam deflection spectroscopy, to examine samples of polycarbonate which had been pyrolyzed in vacuo at various temperatures ranging from 340-750°C. The lowest temperatures, which correspond to the isotherm of the present study, exhibited some mild changes in the infrared spectrum which were comparable to those observed in this study.

One of these changes occurs in the region around 771 cm⁻¹, corresponding to the out-of-plane skeletal vibration of -OCOO- and C-H deformation. Politou observed that this peak showed a decrease in intensity at the lowest temperatures and attributed this to removal of phenol end groups. Referring to schemes set forth by Lee¹¹ and by Davis and Golden (see Chapter 1), the authors conclude that random hydrolysis of the carbonate group, followed by condensation, is occurring during the degradation at these temperatures. A similar change is seen in both materials utilized in this study, see Figure 4.3.2-3 and Figure 4.3.2-4. The intensity of the 771 cm⁻¹ peak definitely decreases with increasing degradation, as seen by Politou. As previously mentioned, all spectra in these and the following figures have been normalized relative to the 1408 cm⁻¹ peak, and curves have been displaced vertically for clarity.

¹⁰ Politou, A. S., C. Morterra, and M. J. D. Low, *Carbon*, **28**, 529, 1990.

¹¹ Lee, L. H., *J. Polym. Sci. Part A*, **2**, 2859, 1964.

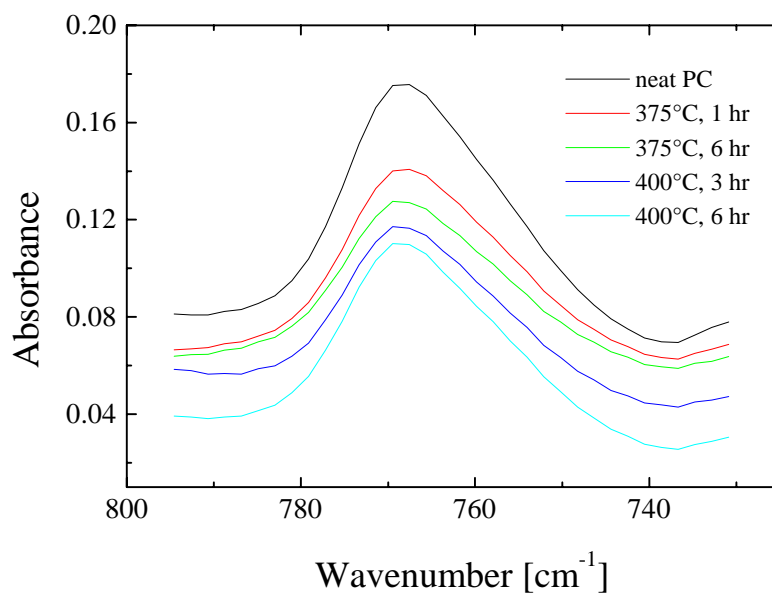


Figure 4.3.2-3 FTIR results for PC(Lab) in the region of the 771 cm⁻¹ peak.

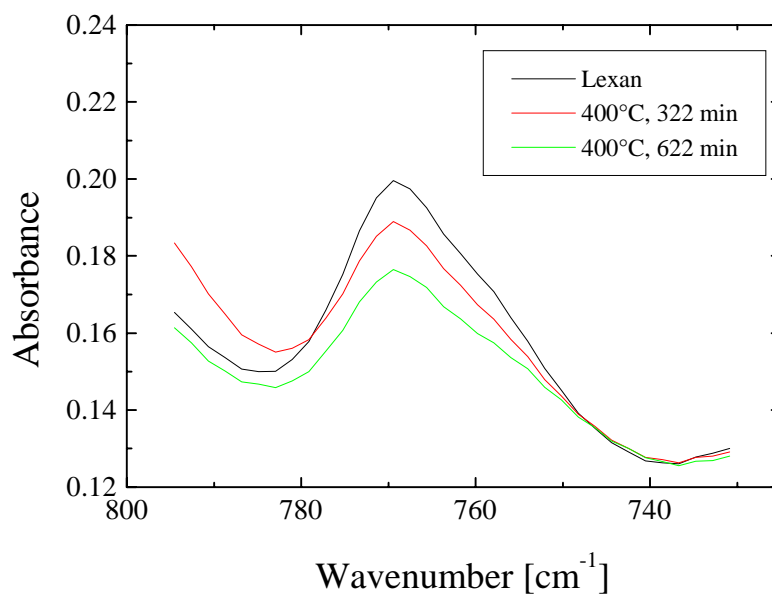


Figure 4.3.2-4 FTIR results for PC(Lex) in the region of the 771 cm⁻¹ peak.

Another spectral region of interest is in the vicinity of the wavenumber of 1778 cm⁻¹, corresponding to C=O stretch of the -OCOO- group. Politou found that this band

decreased in intensity at higher temperatures, finally disappearing completely at around 490°C. This was attributed to scission at the carbonate group. A similar trend was found in this study with small decreases apparent in this peak, as seen in Figure 4.3.2-5 and Figure 4.3.2-6.

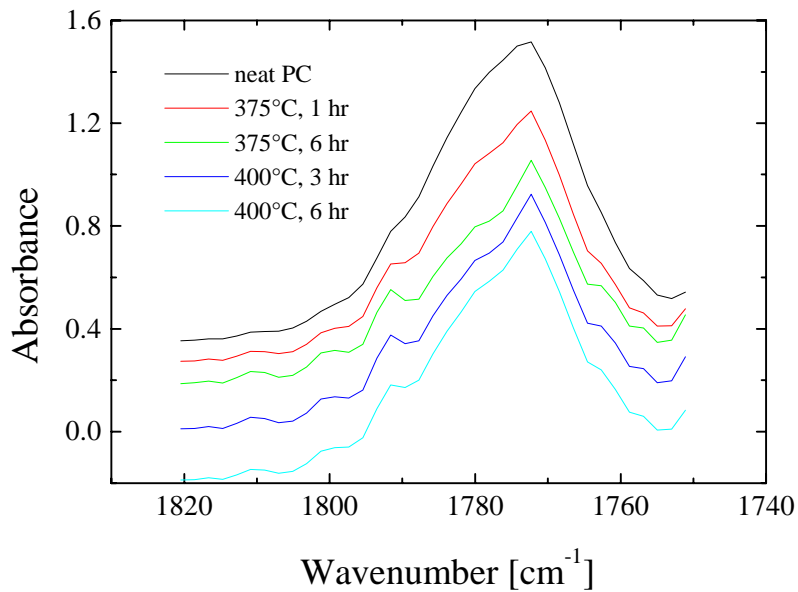


Figure 4.3.2-5 C=O stretching region of the spectra for PC(Lab).

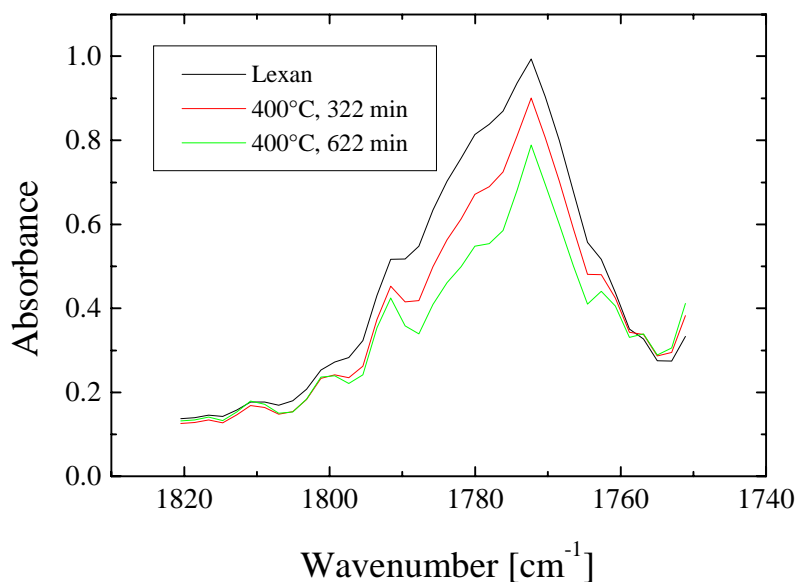


Figure 4.3.2-6 C=O stretching region of the spectra for PC(Lex).

One final spectral region was examined, that of the C-H stretch ($2800\text{-}3200\text{ cm}^{-1}$). It is reported that a decrease in intensity is seen for the -CH_3 -related bands, as well as the appearance of bands at 2924 cm^{-1} and 2862 cm^{-1} when PC degrades at 420°C . For the lower temperatures utilized in the present study, the only change seen in this region, illustrated in Figure 4.3.2-7 and Figure 4.3.2-8, is the decrease of the peak at 2970 cm^{-1} , associated with the CH_3 asymmetrical stretch. It is expected that the other reported changes would be seen with the materials of this study if higher temperatures were used.

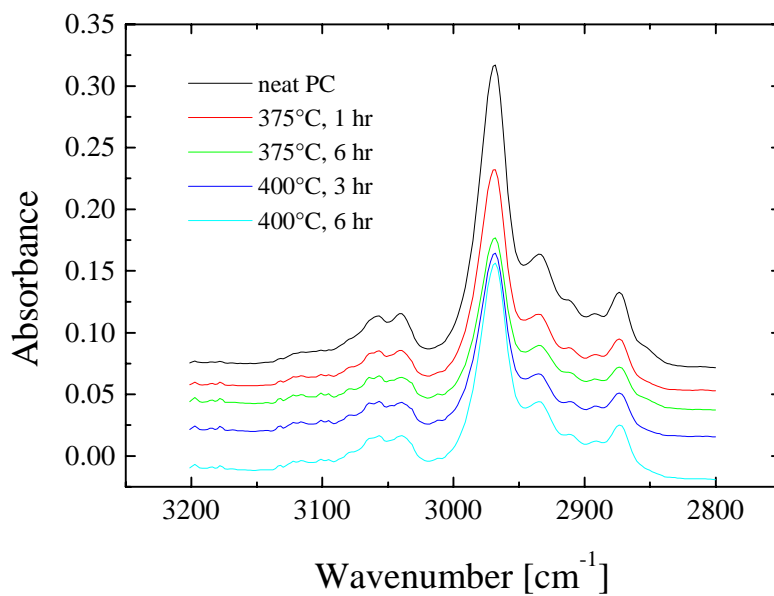


Figure 4.3.2-7 C-H stretching region for PC(Lab).

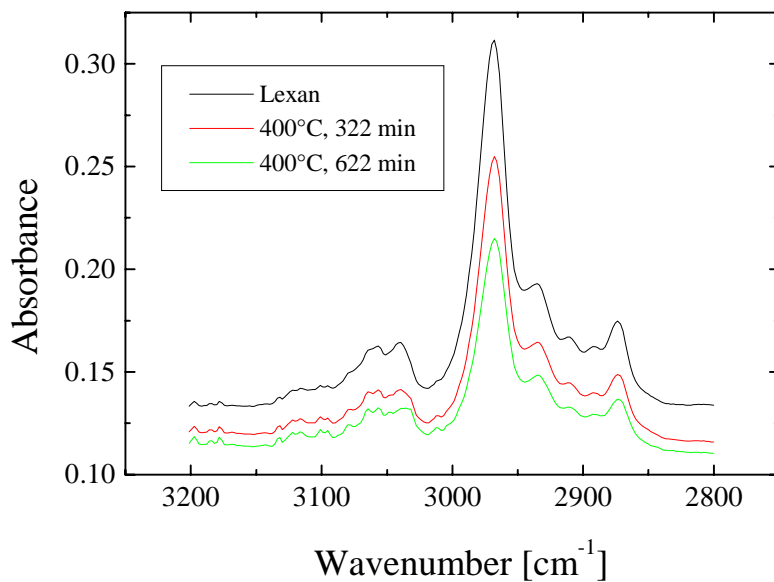


Figure 4.3.2-8 C-H stretching region for PC(Lex).

The infrared data are seen to support the conclusions drawn by Politou and coworkers, which followed from the research of Davis and Golden. Once again, no clear

mechanism can be determined, but the data suggest the presence of scission at both the isopropylidene and carbonate groups. Additionally, these experiments verify that systematic changes are indeed occurring within the samples with increasing levels of degradation, as should be expected.

4.4 Molecular Weight Distribution

4.4.1 GPC Results

Any major chemical change of a polymer, including degradation, usually results in pronounced differences in other parameters of the material, most notably in the key structural feature of the molecular weight distribution. For the polycarbonates of this study, MWD was characterized using gel permeation chromatography as follows. Pieces of the pressed films of the original materials, as well as of degraded samples, were dissolved in *n*-methyl pyrrolidone (NMP) containing 0.02M P₂O₅ at approximately 3 mg/mL. A Waters GPC/ALC 150C instrument equipped with a differential refractometer and an online differential viscometer (Viscotek 150R) in parallel was utilized and allowed absolute molecular weights to be calculated. Columns employed were the Waters μ Styragel HT2 + HT4 + HT5. The flow rate of the mobile phase was 1.0 mL/min, and the injection volume was 100 μ L. Analysis of the resulting data was carried out with TriSEC GPC software (v. 3.0) from Viscotek.

Errors associated with measurements of \overline{M}_w or \overline{M}_n are approximately 10 %. When undegraded PC(Lab) was analyzed in four separate batches, \overline{M}_w ranged from 20700-25800 g/mol with an average value of 22700 ± 2200 g/mol. However, it should be noted here that changes in molecular weight with degradation are often much smaller than this error. For example, PC(Lab) degraded at 325°C for 3 hours demonstrates a weight average molecular weight of 19900 g/mol which represents a difference of 1800 g/mol relative to the undegraded \overline{M}_w . The change in molecular weight between these two samples is thus less than the error associated with the measurement itself. Consequently, scatter in the data is expected and cannot be alleviated as long as GPC is involved. Unfortunately, not all the samples for the present study were analyzed in one batch, so

any changes to the instrument or columns in the intervening time would also subsequently affect the results. Clearly, an ideal situation would be to have an instrument dedicated to a single polymer with columns perhaps more closely matched to the expected molecular weights.

Another key factor leading to the GPC error involves data analysis. The software requires the user to draw a baseline as well as choose the limits of integration for the peak in the curve. It has been found that small changes in either of these two properties leads to changes in the resulting molecular weights. These absolute differences are not large, but in the context of the small changes under investigation, they are significant. Thus, some of the scatter which will be seen in the final data can be attributed to random error in analysis of the data.

Molecular weight distributions, calculated from the GPC results, are shown in Figure 4.4.1-1-Figure 4.4.1-5 for PC(Lab) and in Figure 4.4.1-6 for PC(Lex). It should be noted that the curves tend to broaden in a symmetrical manner at the lower levels of degradation. At higher degradations, such as 350°C for 24 hr, 375°C for 24 hr, and 400°C for 12 hr, the curves are skewed towards the lower molecular weights, as would be expected. In general, the trend was to shift the MWD toward a lower average molecular weight with increasing thermal exposure. At the highest level of degradation (400°C, 12 hr, Figure 4.4.1-5), the presence of multiple peaks is observed denoting that the distribution is trimodal. This may indicate that there is some low molecular weight species present, as well as polymer with a bimodal distribution of molecular weight. Another feature to note is the decreasing heights of the curves of PC(Lab) as the degradation proceeds, particularly at the highest levels of 375 and 400°C (see Figure 4.4.1-4 and Figure 4.4.1-5).

Conversely, in addition to the data exhibiting more noise for PC(Lex), those GPC curves also decrease in height but then show an increase at the highest thermal exposure levels. This trend should be taken with caution since the GPC curves were not as smooth as would be expected and because it is unclear what effect the addition of the stabilizer in the PC(Lex) has on the degradation and subsequent property changes. Furthermore, one will recall that, for the FTIR work with methylene chloride, these two most degraded samples did not fully dissolve, which may imply excessive charring or crosslinking.

While this lack of dissolution was not observed with NMP solvent, it still may be possible that these last two samples are somehow exhibiting misleading results. It is also worth noting that these levels of degradation are quite extreme and are unlikely to be encountered in the normal use of this polymer. However, these extreme conditions were chosen to fully illustrate the trends which were expected in this study.

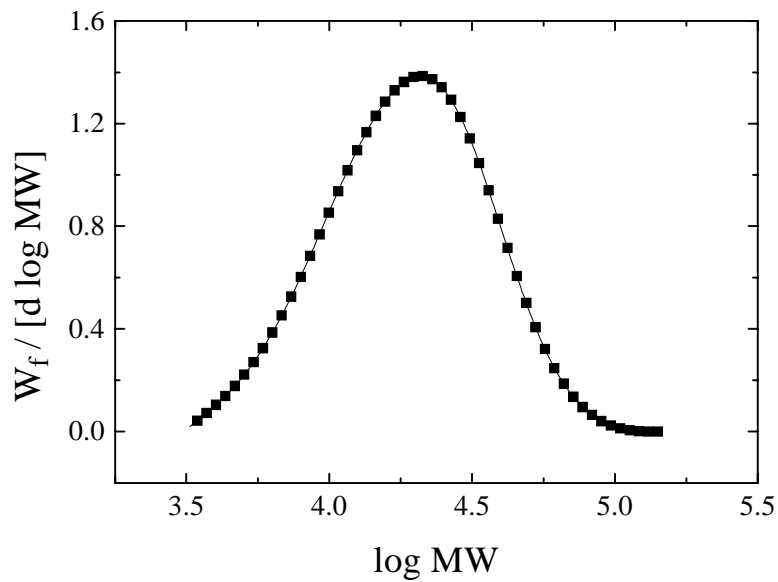


Figure 4.4.1-1 Molecular weight distribution for PC(Lab).

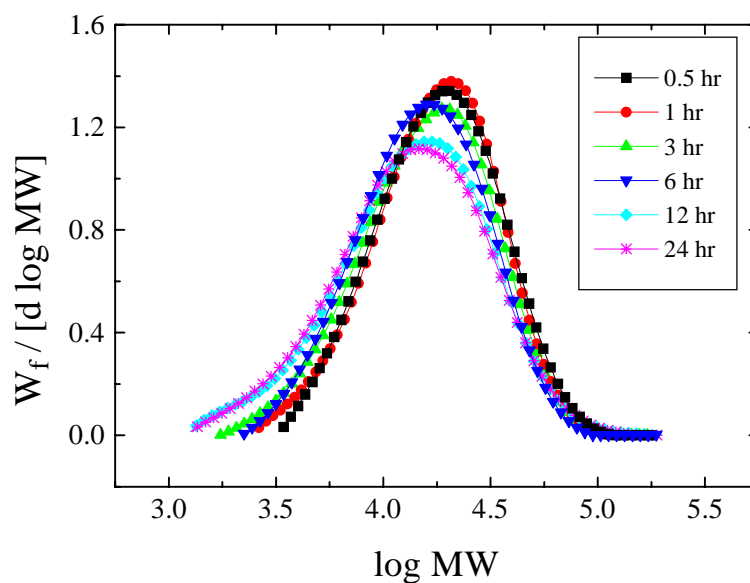


Figure 4.4.1-2 Molecular weight distributions for PC(Lab) degraded at 325°C for the times indicated.

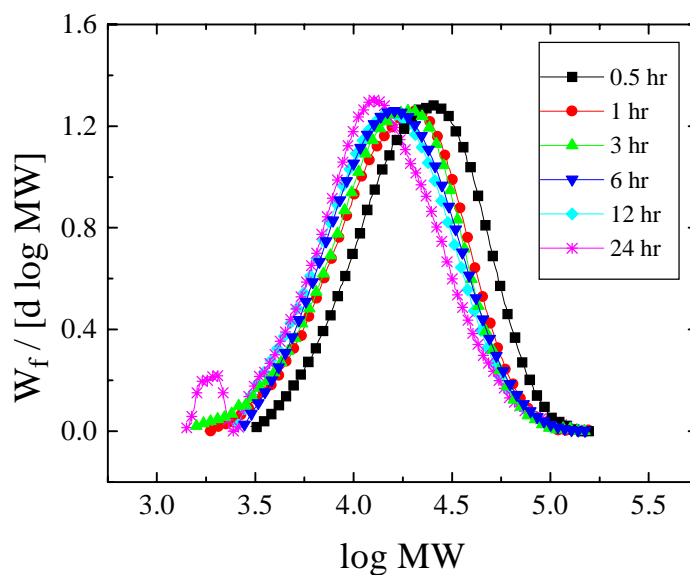


Figure 4.4.1-3 Molecular weight distributions for PC(Lab) degraded at 350°C for the times indicated.

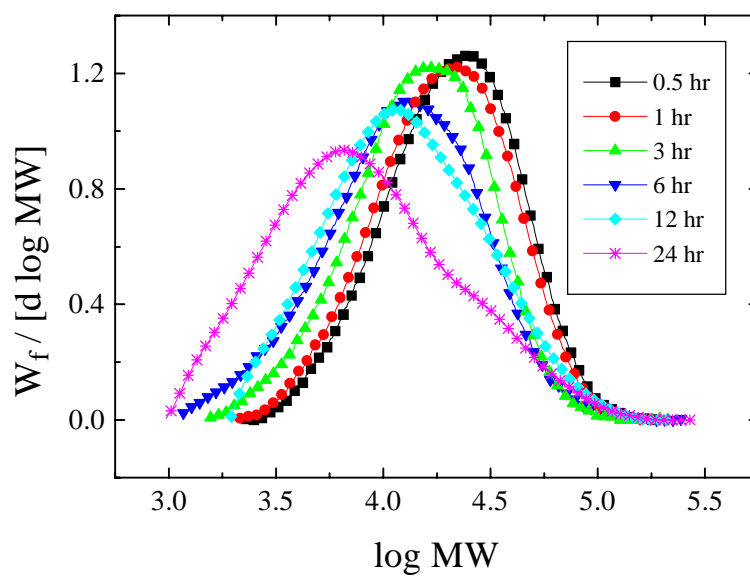


Figure 4.4.1-4 Molecular weight distributions for PC(Lab) degraded at 375°C for the times indicated.

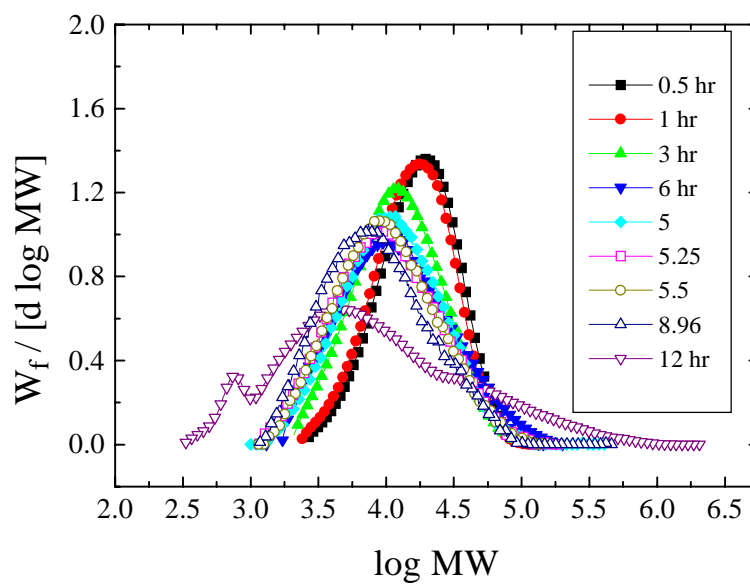


Figure 4.4.1-5 Molecular weight distributions for PC(Lab) degraded at 400°C for the times indicated.

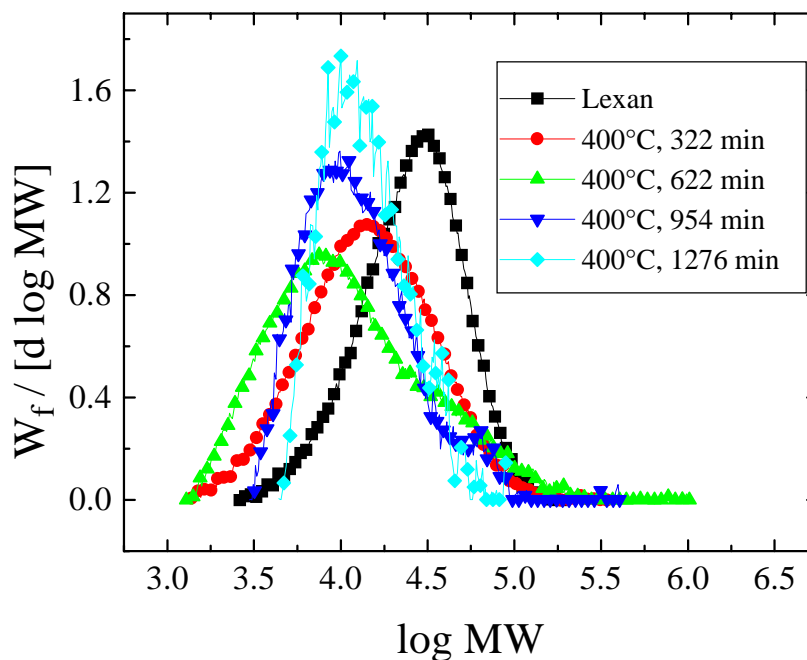


Figure 4.4.1-6 Molecular weight distributions for PC(Lex).

4.4.2 Molecular Weight Analysis

If the degradation is indeed first order, a plot of τ versus the reciprocal of the number average molecular weight should yield a straight line. This response can be seen in Figure 4.4.2-1 for PC(Lab) and in Figure 4.4.2-2 for PC(Lex) (with the highest degrees of degradation excluded from the linear fit), confirming once again that first order kinetics hold here. Additionally, this relationship provides a mathematical model between τ and the number average molecular weight, which can be used to predict values of \bar{M}_n with a known thermal history. It is also of interest to see if any trend exists when either weight average or number average molecular weights are plotted as functions of time. In Figure 4.4.2-3 and Figure 4.4.2-4, one can see the results of these graphs for PC(Lab). The trend for the weight average values is essentially as would be expected, with a decrease in \bar{M}_w with increasing time or temperature. The number average values are less regular, but this may be due in part to the sources of error in GPC discussed previously. It should be noted that, in Figure 4.4.2-4, the value for the sample degraded

at 325°C for 6 hours is somewhat higher than expected, and consequently, any other fits which utilize this value will exhibit more deviation when that point is included. Similar results for PC(Lex) are illustrated in Figure 4.4.2-5 and Figure 4.4.2-6. In contrast, the number average values for PC(Lex) do not follow the well-defined trend observed for \bar{M}_w . This may be due in part to the extremely high degree of degradation, as mentioned previously. The numerical values for weight and number average molecular weights, as well as the polydispersity, are shown in Table 4.4-1 for all samples. It should also be noted that the polydispersity index is generally approaching 2 as the degradation proceeds, which is also consistent with a first order reaction and random scission of the molecules. Once again, though, any trend for the commercial polymer is not as evident as for the laboratory grade material. These differences may be partially attributable to the presence of the stabilizer in PC(Lex), as well as to the higher initial molecular weight of these samples.

Table 4.4-1

Summary of Molecular Weight Data for All Samples

Sample	\bar{M}_w [g/mol]	\bar{M}_n [g/mol]	PDI
PC(Lab)	22500	15200	1.48
325°C-0.5 hr	22000	14700	1.50
-1 hr	21400	14000	1.53
-3 hr	20900	13900	1.50
-6 hr	20900	13900	1.50
-12 hr	18400	9700	1.90
-24 hr	18000	9520	1.90
350°C-0.5 hr	21300	14400	1.65
-1 hr	21000	12900	1.60
-3 hr	20000	13100	1.53
-6 hr	19200	11400	1.68
-12 hr	18600	11500	1.62
-24 hr	17200 (2 peaks)	9470	1.82
375°C-0.5 hr	21000	14500	1.45
-1 hr	19600	13400	1.46
-3 hr	19100	12600	1.52
-6 hr	17000	8670	1.96
-12 hr	15500	7730	2.01
-24 hr	13500	5780	2.34
400°C-0.5 hr	20900	13600	1.54
-1 hr	19000	12400	1.53
-3 hr	15800	9400	1.68
-5 hr	15200	7860	1.93
-5.25 hr	14700	7030	2.09
-5.5 hr	14200	7140	1.99
-6 hr	15400	7550	2.04
-8.96 hr	12500	6030	2.07
PC(Lex)	30900	19700	1.57
400°C-5.37 hr	21000	10300	2.04
-10.37 hr	20400	7270	2.81
-15.9 hr	17100	10000	1.71
-21.27 hr	16000	11900	1.34

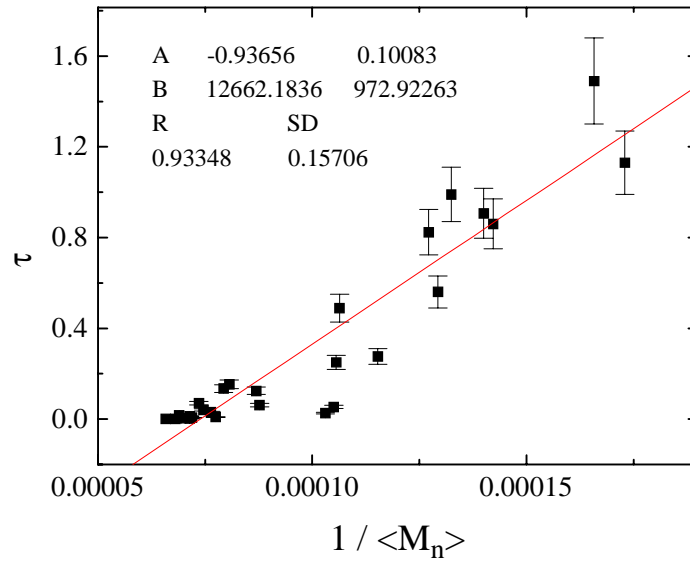


Figure 4.4.2-1 Influence of exposure time on number average molecular weight for PC(Lab).

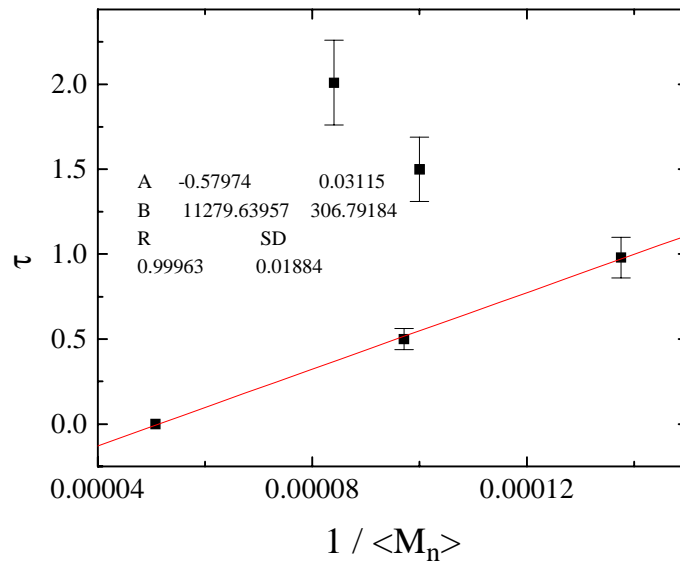


Figure 4.4.2-2 Influence of exposure time on number average molecular weight for PC(Lex).

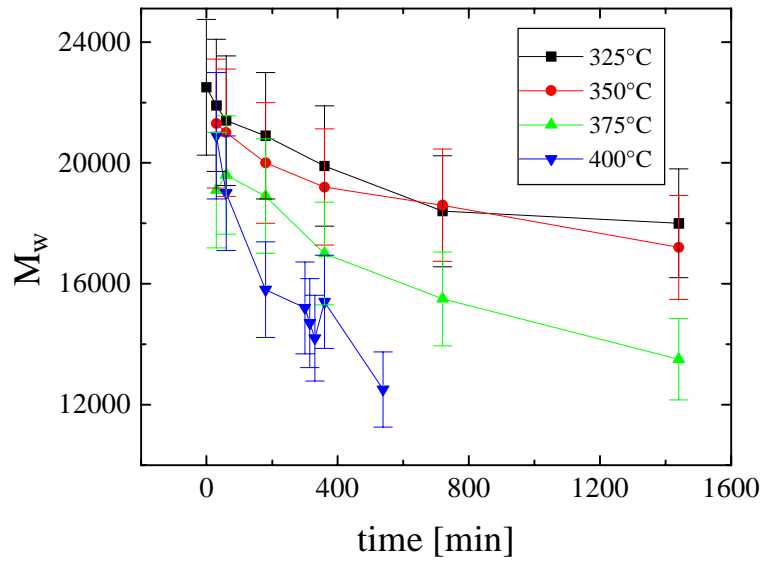


Figure 4.4.2-3 Influence of exposure time on weight average molecular weight for PC(Lab).

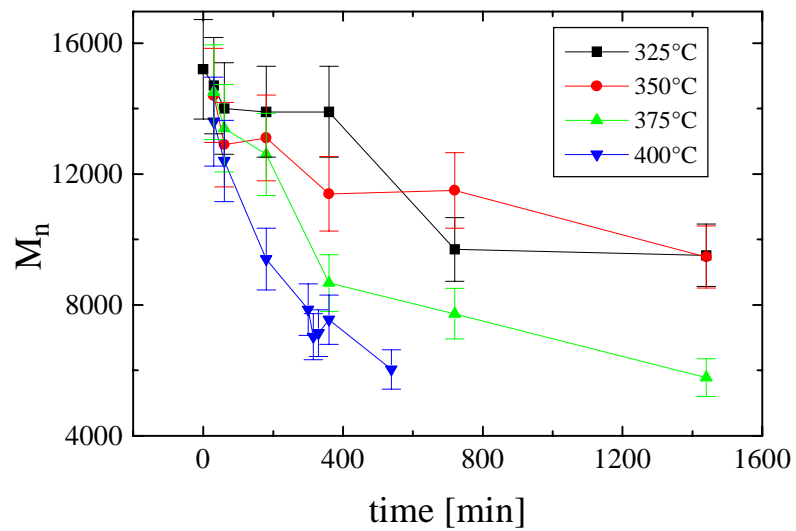


Figure 4.4.2-4 Influence of exposure time on number average molecular weight for PC(Lab).

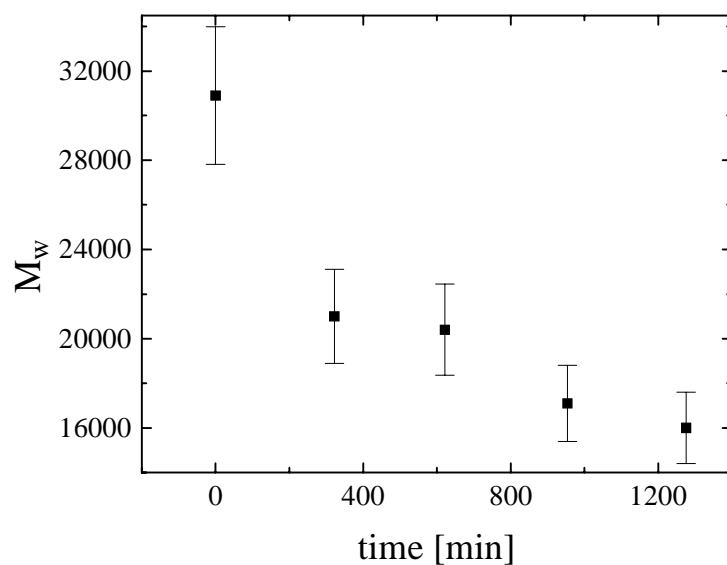


Figure 4.4.2-5 Influence of exposure time on weight average molecular weight for PC(Lex).

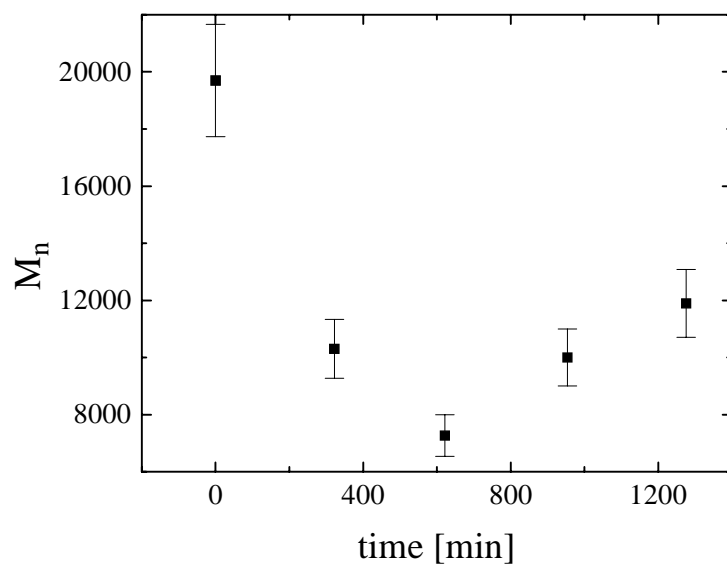


Figure 4.4.2-6 Influence of exposure time on number average molecular weight for PC(Lex).

4.4.3 MWD Superposition

As mentioned above, Chan and Balke recently recognized the utility of molecular weight distribution superposition based on the reduced time, τ , the degree of degradation. They showed that two different samples with equal values of τ , would have exactly the same molecular weight distributions in support of their theory. This methodology was applied to the PC(Lab) samples of this present study. Results are illustrated in Figure 4.4.3-1-Figure 4.4.3-3. In the first molecular weight distributions for samples degraded at 325°C for 12 hours ($\tau = 0.026$) and at 350°C for 3 hours ($\tau = 0.030$) are presented. Clearly, the curves superpose quite well, lending support to the theory. The next figure, which shows samples degraded at 350°C for 12 hours ($\tau = 0.12$) and at 375°C for 3 hours ($\tau = 0.13$), also demonstrates the similarity of the two results, although the replication is not as precise as in the previous case. For purposes of comparison, and to show that a different τ does indeed signify a different distribution, this figure also includes the distribution for a sample degraded at 325°C for 1 hr ($\tau = 1.46e-3$). Clearly, there is differentiation among samples with varying degrees of degradation. Similarly, Figure 4.4.3-3 illustrates the distributions for samples degraded for 375°C for 6 hours ($\tau = 0.28$) and 350°C for 12 hours ($\tau = 0.25$). Once again, the curves do not superpose exactly; but, it should also be noted that the τ values are not identical, so some differences would be expected. Furthermore, the sources of error discussed previously play some part here.

Chan and Balke used data similar to those just discussed to calculate Williams-Landel-Ferry parameters C_1 and C_2 from shift factors. They started with the equation

$$\tau(t, T) = \tau\left(\frac{t}{a_T^0}, T_0\right) \quad \text{Eqn. 4.4-1}$$

and applied it to points with the same τ values and thereby calculated two values for a_T^0 . These two numbers were then used in the WLF equation,

$$\log a_T^0 = \frac{-C_1^0(T - T_0)}{(C_2^0 + T - T_0)} \quad \text{Eqn. 4.4-2}$$

to find values for C_1^0 and C_2^0 . In the same manner, a reference temperature can be chosen for the data of the present study, and is taken to be 350°C. Two different shift

factors can be calculated from the three conditions where τ is the same, yielding $a_{375}^0 = 0.25$ and $a_{400}^0 = 0.083$. These two numbers yield WLF constants of $C_1^0 = 5.2$ and $C_2^0 = 191$ K. It is unclear, however, what usefulness these numbers may have for predicting molecular weight distributions knowing the thermal history. But, this discussion is included to illustrate the methodology and power of such an approach. Further, caution should be applied when using these numbers as they are the product of only two data points.

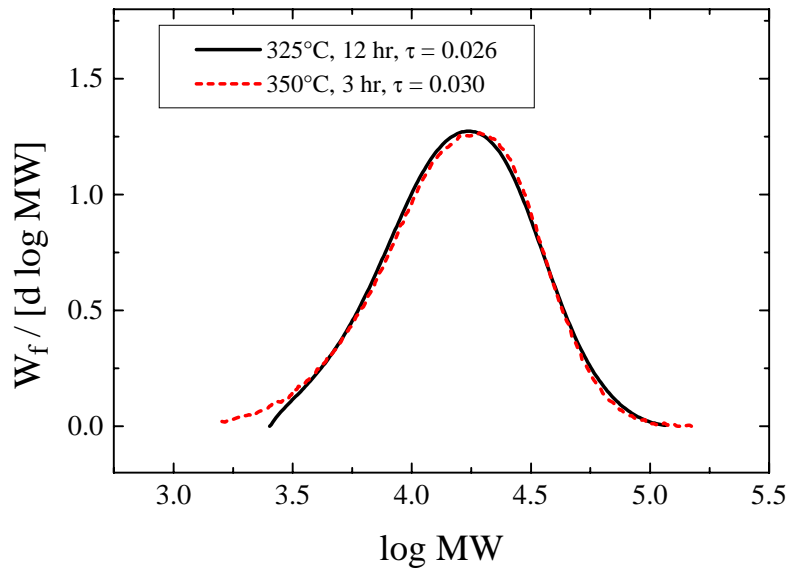


Figure 4.4.3-1 Comparison of molecular weight distributions for samples with similar τ values.

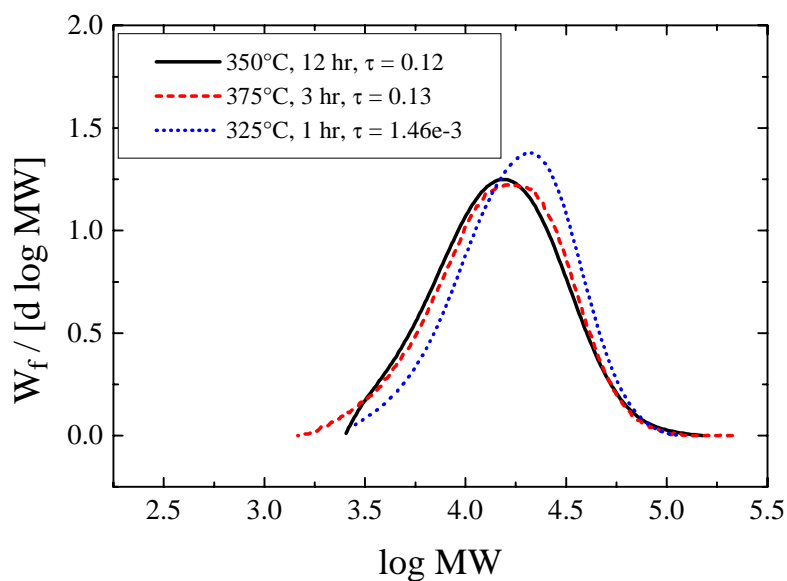


Figure 4.4.3-2 Comparison of molecular weight distributions for samples with similar τ values.

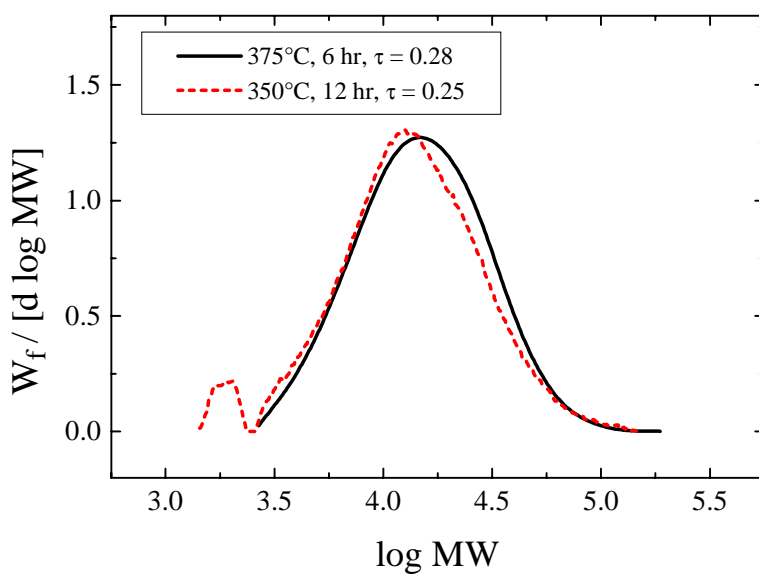


Figure 4.4.3-3 Comparison of molecular weight distributions for samples with similar τ values.

Although Chan and Balke first published this superposition methodology for degradation, they did not take the logical next step of creating a master curve for these

MWDs. Such an exercise requires MWDs for isothermally degraded samples in order to shift the data. Since isotherms were used for the present degradations, these temperatures will also be utilized for the MWD master curve. In order to find values for the isotherm, the assumption was made that the MWDs were broadening in a symmetric manner. This was shown to be true, at least for the majority of the samples, previously. Then the x-axis value of the peak of the molecular weight distribution curve was taken as one coordinate for each sample of a particular isothermal degradation. The isotherms produced in this fashion, one for each degradation temperature, were all then plotted versus τ . It should be recalled that τ represents a reduced time. As was seen previously in Figure 4.4.3-1-Figure 4.4.3-3, samples with identical values of τ should exhibit overlaying MWDs. Therefore, when the isotherms are all plotted versus τ in the same graph, the four curves collapse onto a single curve without the need for manual shifting of the curves, as seen in Figure 4.4.3-4. The appropriate errors are shown for τ , but it is not possible, with only two sets of data, to calculate errors for the molecular weight distributions and thus peak values. The results show that, within the errors, the curves exhibit reasonable superposition. Such a graph enables a researcher to read off a peak quantity for any value of τ (regardless of temperature), and then shift the distribution curve along the x-axis such that its peak is at the value read from the master curve. Thus the molecular weight distribution is predicted for that specimen without having to perform the GPC measurements. From such information properties such as impact strength, T_g , tensile strength, and rheological features might be predicted. The caveat, though, is that broadening of the curves must be minimal and symmetric, or this method fails. However, since such a scheme is original with this thesis, these preliminary data are to be regarded as encouraging, and future refinements will undoubtedly lead to better fits. Furthermore, more sophisticated scenarios may be able to make use of the WLF parameters approach. One additional problem which must be solved is that of the scaling of the heights of the curves. These height changes may be due to the filtering off of crosslinked gel fractions prior to GPC analysis, or to a decrease in the refractive index increment difference for the polymer in the solvent due to changes in the polymer chemical composition. In either case, as discussed previously, the peak heights tend toward lower values as the degradation becomes more extreme. It is felt that future work with this methodology will

shed more light on how these height changes can be predicted and increase the accuracy of the model.

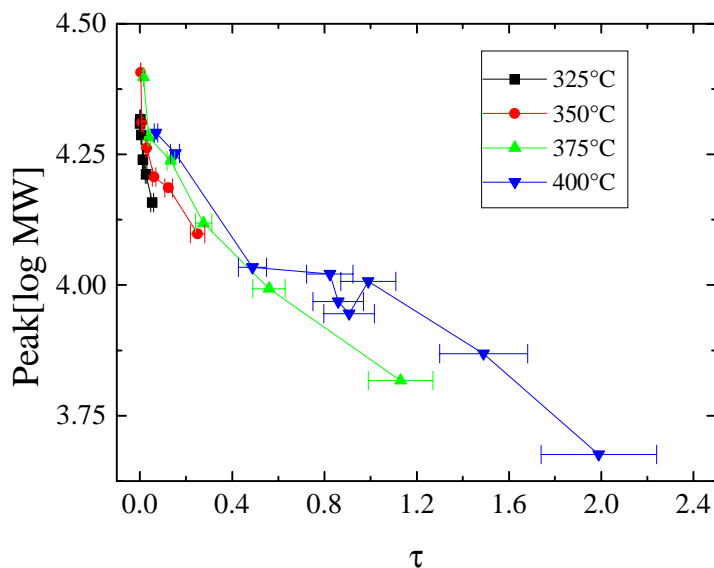


Figure 4.4.3-4 Molecular weight distribution master curve for PC(Lab).

From the obtained data, it is clear that τ , the degree of degradation, can be related to MWD. Not only is τ inversely related to the number average molecular weight, but it can also be used to predict the peak in the molecular weight distribution curve via the master curve as in Figure 4.4.3-4, leading to a molecular weight distribution at any degree of degradation. As will be detailed in Chapter 5, \bar{M}_n can be linked to various other properties of interest through structure-property relationships found in the literature, so knowledge of this molecular weight can lead to prediction of other parameters. Thus, Chan and Balke's method has been affirmed and extended with prediction of the molecular weights directly related to τ .